

## Strontiohurlbutite, SrBe<sub>2</sub>(PO<sub>4</sub>)<sub>2</sub>, a new mineral from Nanping No. 31 pegmatite, Fujian Province, Southeastern China

CAN RAO<sup>1,2,\*</sup>, RUCHENG WANG<sup>1</sup>, FRÉDÉRIC HATERT<sup>3</sup>, XIANGPING GU<sup>4</sup>, LUISA OTTOLINI<sup>5</sup>, HUAN HU<sup>1</sup>, CHUANWAN DONG<sup>2</sup>, FABRICE DAL BO<sup>3</sup> AND MAXIME BAIJOT<sup>3</sup>

<sup>1</sup>State Key Laboratory for Mineral Deposits Research, School of Earth Sciences and Engineering, Nanjing University, Nanjing 210093, P.R. China

<sup>2</sup>Department of Earth Sciences, Zhejiang University, Hangzhou 310027, P.R. China

<sup>3</sup>Laboratoire de Minéralogie, B18, Université de Liège, B-4000 Liège, Belgium

<sup>4</sup>School of Earth Sciences and Info-physics, Central South University, Changsha, Hunan 410083, P.R. China

<sup>5</sup>C.N.R.-Istituto di Geoscienze e Georisorse (IGG), Unità di Pavia, Via A. Ferrata 1, I-27100 Pavia, Italy

### ABSTRACT

Strontiohurlbutite, ideally SrBe<sub>2</sub>(PO<sub>4</sub>)<sub>2</sub>, is a new member of hurlbutite group discovered in the Nanping No. 31 pegmatite, Fujian province, southeastern China. Crystals are mainly found in zones I, II, and IV; they are platy, subhedral-to-anhedral, with a length from 5 μm to 1.5 mm. Associated minerals mainly include quartz, muscovite, beryl, hurlbutite, hydroxylherderite, apatite-group minerals, and phenakite. Strontiohurlbutite crystals are light blue, translucent-to-transparent, and have vitreous luster. The Mohs hardness is about 6, and the tenacity is brittle. Optically, strontiohurlbutite is biaxial (–), α = 1.563(3), β = 1.569(2), γ = 1.572(3) (white light), 2V<sub>meas</sub> = 68.5(5)°, and exhibits weak dispersion, r > v. The optical orientation is X = b, Y ≈ c. Electron-microprobe and SIMS analyses (average of 16) give SrO 29.30, P<sub>2</sub>O<sub>5</sub> 51.05, CaO 0.91, BaO 0.64, and BeO 17.71 wt%; total 99.61 wt%. The empirical formula, based on 8 O apfu, is (Sr<sub>0.81</sub>Ca<sub>0.05</sub>Ba<sub>0.01</sub>)<sub>Σ0.87</sub>Be<sub>2.02</sub>P<sub>2.05</sub>O<sub>8</sub>. The stronger eight lines of the measured X-ray powder-diffraction pattern [*d* in Å(*I*)(*hkl*)] are: 3.554(100)(121); 3.355(51)(211); 3.073(38)(022); 2.542(67)(113); 2.230(42)(213); 2.215(87)(32 $\bar{1}$ ); 2.046(54)(223); 1.714(32)(143). Strontiohurlbutite is monoclinic, space group *P*2<sub>1</sub>/*c*; unit-cell parameters refined from single-crystal X-ray diffraction data are: *a* = 7.997(3), *b* = 8.979(2), *c* = 8.420(7) Å, β = 90.18(6)°, *V* = 604.7(1) Å<sup>3</sup> (*Z* = 4, calculated density = 3.101 g/cm<sup>3</sup>). The mineral is isostructural with hurlbutite, CaBe<sub>2</sub>(PO<sub>4</sub>)<sub>2</sub>, and with paracelsian, BaAl<sub>2</sub>Si<sub>2</sub>O<sub>8</sub>. The formation of strontiohurlbutite is related to the hydrothermal alteration of primary beryl by late Sr- and P-rich fluids.

**Keywords:** Strontiohurlbutite, SrBe<sub>2</sub>(PO<sub>4</sub>)<sub>2</sub>, new mineral, hurlbutite, Nanping No. 31 pegmatite, Fujian province, China

### INTRODUCTION

The new mineral strontiohurlbutite, a Sr-dominant analog of hurlbutite, was discovered in the Nanping No. 31 pegmatite, Fujian province, southeastern China. Polarizing microscopy, electron-microprobe analyses, X-ray diffraction measurements, Raman spectroscopy, and secondary-ion mass spectrometry (SIMS), were used to determine its petrographic features, chemical composition, and crystal structure. The species and the name have been approved by the International Mineralogical Association, Commission on New Minerals, Nomenclature and Classification (CNMNC) (IMA 2012-032) (Williams et al. 2012). The co-type specimen used for the electron-microprobe analyses, X-ray powder diffraction, XPS, Raman, and optical measurements is deposited at the Geological Museum of China, Beijing, China, catalog number M11803. The co-type sample used for the single-crystal structure measurements is stored at the Laboratory of Mineralogy, University of Liège, catalog number 20387. This paper presents the occurrence of this new Sr phosphate with the hurlbutite-type structure, and discusses the origin of strontiohurlbutite in the Nanping pegmatite.

\* E-mail: canrao@zju.edu.cn

### OCCURRENCE AND PARAGENESIS

Strontiohurlbutite was found in the Nanping No. 31 pegmatite, Fujian Province, southeastern China, which is located at longitude E 118°06', latitude N 26°40', about 8 km west of the Nanping city. The No. 31 pegmatite is a highly evolved and well-zoned pegmatite in the Nanping pegmatite district. Five discontinuous mineralogical-textural zones were distinguished from the outermost zone inward (Yang et al. 1987): quartz – albite – muscovite zone (Zone I), saccharoidal albite ± muscovite zone (Zone II); quartz – coarse albite – spodumene zone (Zone III); quartz – spodumene – amblygonite zone (Zone IV); and blocky quartz – K-feldspar zone (Zone V). The petrography and mineral paragenesis of different textural zones in this pegmatite have been well described in previous publications (e.g., Yang et al. 1987; Rao et al. 2009, 2011). Strontiohurlbutite was found in samples from zones I, II, and IV.

Strontiohurlbutite from zone I forms subhedral to euhedral crystals up to 1.5 mm long, mainly in close association with quartz (Fig. 1a). Backscattered electron (BSE) images show the crystals to be weakly heterogeneous (Fig. 1a), and the brighter areas are slightly richer in Sr than the darker areas. Other associated minerals include muscovite, fluorapatite, and hurlbutite. In

zone II, strontiohurlbutite occurs as small aggregates about 5 to 100  $\mu\text{m}$  across. They are closely associated with beryl, hurlbutite, hydroxylherderite, fluorapatite, and phenakite, forming the Be silicate + phosphate mineral associations interstitial to albite crystals (Fig. 1b; Rao et al. 2011, their Fig. 4a, the brightest areas). In zones I and IV, strontiohurlbutite also forms aggregates with a size ranging from 2 to 50  $\mu\text{m}$ ; it surrounds hurlbutite crystals from zone I, and is distributed along the fractures of Cs-rich beryl from zone IV (Fig. 1c). Other secondary phases observed in this aggregates include beryl, hurlbutite, hydroxylapatite, and muscovite.

### PHYSICAL AND OPTICAL PROPERTIES

Strontiohurlbutite forms platy, subhedral crystals and anhedral grains. More than 50 grains were found in zones I and II; they are light blue, transparent to translucent, and have vitreous luster. The Mohs hardness is about 6, the tenacity is brittle, and no cleavage was observed. The calculated density, based on the empirical formula and single-crystal unit-cell parameters, is 3.101  $\text{g}/\text{cm}^3$ . Optically, strontiohurlbutite is biaxial negative, with  $\alpha = 1.563(2)$ ,  $\beta = 1.569(2)$ ,  $\gamma = 1.572(3)^\circ$ , measured in white light. The  $2V$  angle, measured directly by conoscopic observations, is  $68.5(5)^\circ$ ; the calculated  $2V$  is  $70^\circ$ . It exhibits weak dispersion,  $r > v$ , and it is colorless. The optical orientation is  $X = \mathbf{b}$ ,  $Y \approx \mathbf{c}$ , and pleochroism is absent. Based on the calculated density and the measured indices of refraction, the compatibility index [ $1 - (K_p/K_c)$ ] is  $-0.006$ , and corresponds to the "Superior" category (Mandarino 1981).

### RAMAN SPECTROSCOPY

Raman spectra of strontiohurlbutite were collected using a Renishaw RM2000 Laser Raman microprobe in the State Key Laboratory for Mineral Deposits Research at Nanjing University. A 514.5 nm  $\text{Ar}^+$  laser with a surface power of 5 mW was used for exciting the radiation. Silicon ( $520 \text{ cm}^{-1}$  Raman shift) was used as a standard. Raman spectra were acquired from 100 to 1000  $\text{cm}^{-1}$  and the accumulation time of each spectrum is 60 s. Raman spectra were collected on single crystals of strontiohurlbutite on polished thin section chips. Figure 2 shows the Raman spectrum of strontiohurlbutite, which is remarkably similar to the spectrum of hurlbutite, confirming the structural similarity between strontiohurlbutite and hurlbutite. The Raman spectrum contains strong sharp peaks at  $1022 \text{ cm}^{-1}$ ; medium sharp peaks at 587, 575, 550, 442, 343, and  $204 \text{ cm}^{-1}$ ; and weak sharp peaks at 1178, 1135, 492, 421, and  $176 \text{ cm}^{-1}$ , respectively. The Raman shifts of  $(\text{PO}_4)$  groups were observed at  $1022 (v_1)$ , 421, 442 ( $v_2$ ), 1135, 1178 ( $v_3$ ), and 550, 575, and  $587 \text{ cm}^{-1} (v_4)$ . The Be-O vibration modes are probably at 204 and  $492 \text{ cm}^{-1}$ , and the Raman shifts at 176 and  $343 \text{ cm}^{-1}$  certainly correspond to Sr-O vibrations.

### CHEMICAL COMPOSITION

The chemical composition of strontiohurlbutite (Table 1) was obtained with a JEOL JXA-8100M electron microprobe (WDS mode, 15 kV, 20 nA, beam diameter 1  $\mu\text{m}$ ) at the State Key Laboratory for Mineral Deposits Research, Nanjing University. The following standards were used: synthetic  $\text{Ba}_3(\text{PO}_4)_2$  ( $\text{BaLa}$ ,  $\text{PK}\alpha$ ), synthetic  $\text{SrSO}_4$  ( $\text{SrLa}$ ), and hornblende ( $\text{CaK}\alpha$ ).

To determine the BeO content of strontiohurlbutite, SIMS

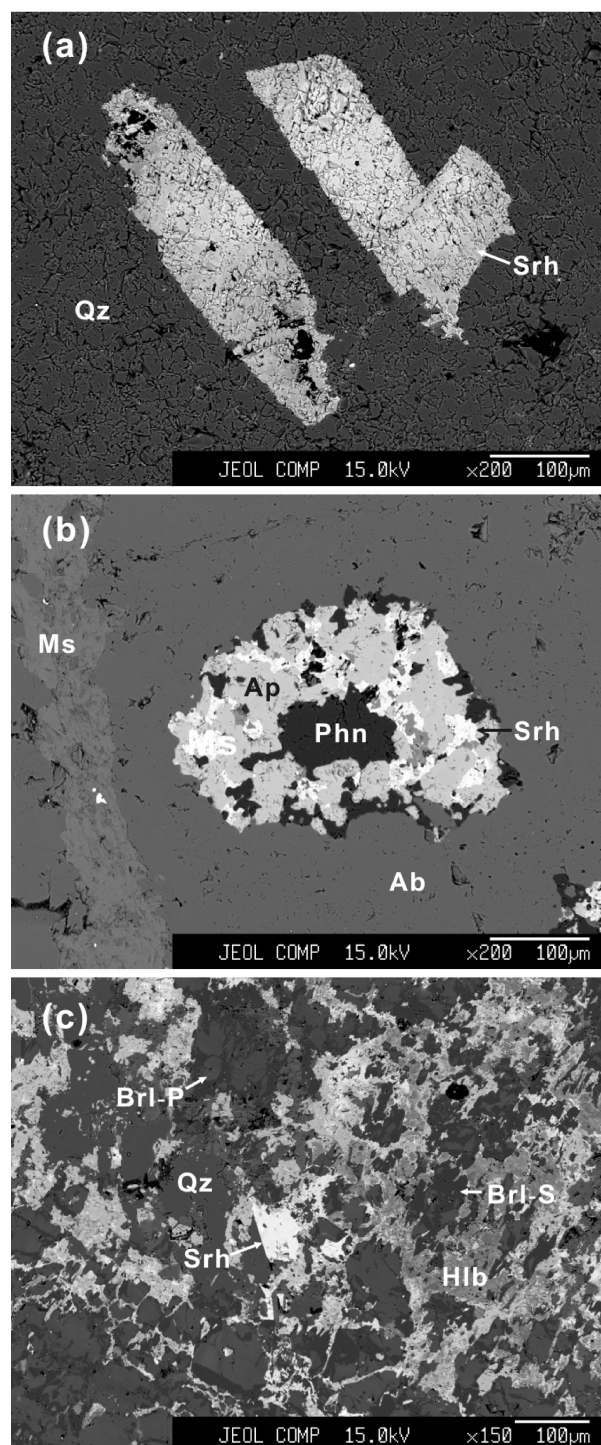


**FIGURE 1.** BSE images showing occurrence and mineral associations of strontiohurlbutite. (a) Euhedral strontiohurlbutite crystals in close association with quartz in zone I. (b) Small aggregate of strontiohurlbutite in a Be silicate + phosphate assemblage interstitial to albite crystals in zone II. (c) Strontiohurlbutite associated with secondary phases (beryl, hurlbutite, hydroxylapatite, and muscovite) in the fractures of primary beryl from zone IV. Abbr.: Qz = quartz, Srh = strontiohurlbutite, Brl-P = primary beryl, Brl-S = secondary beryl, Phn = phenakite, Ab = albite, Hlb = hurlbutite, Ms = muscovite, Ap = apatite.

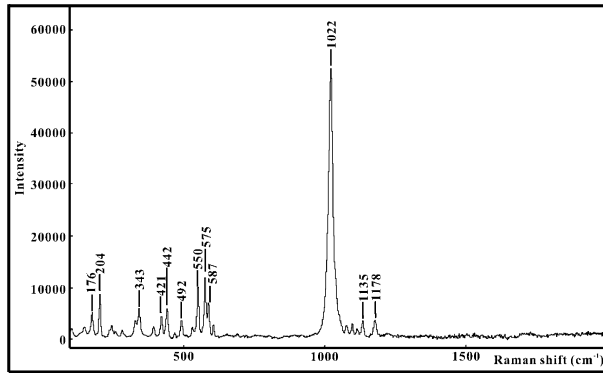


FIGURE 2. The Raman spectrum of strontiohurlbutite.

measurements were performed with a Cameca IMS-4F ion microprobe installed at CNR-IGG, Pavia (Italy). The experimental conditions are similar to those reported in the literature (Ottolini et al. 1993, 2002; Hatert et al. 2011). We selected a sample of beryllonite (courtesy of S. Philippo, Natural History Museum of Luxembourg) as standard for Be. The calibration factor for Be in the standard was obtained through the calculation of the experimental Be ion yield, having chosen P as the inner element for the matrix. We thus derived the IY(Be/P), defined as  $(\text{Be}^+/\text{P}^+)/[(\text{Be}(\text{at})/\text{P}(\text{at}))]$  where  $\text{Be}^+$  and  $\text{P}^+$  are the current intensities detected at the electron multiplier and (at) is the elemental atomic concentration. The IY (Be/P) was then used to calculate the Be concentration in the strontiohurlbutite, resulting in  $17.71 \pm 0.464(1\sigma)$  BeO wt%. Additionally, a few H<sub>2</sub>O about  $0.066 \pm 0.010(1\sigma)$  wt% is detected in strontiohurlbutite; lithium is absent.

Representative analyses of strontiohurlbutite (Table 1) lead to the empirical formula  $(\text{Sr}_{0.81}\text{Ca}_{0.05}\text{Ba}_{0.01})_{\Sigma 0.87}\text{Be}_{2.02}\text{P}_{2.05}\text{O}_8$ , based on 8 O atoms per formula unit. The idealized, end-member formula is  $\text{SrBe}_2(\text{PO}_4)_2$ , which requires 35.06 wt% SrO, 16.92 wt% BeO, and 48.02 wt% P<sub>2</sub>O<sub>5</sub>; total 100.00 wt%. A careful examination of chemical data (Table 1) indicates significant amounts of Ca and Ba, reaching 3.10 wt% CaO and 0.22 wt% BaO, in strontiohurlbutite from zone IV. This indicates the existence of a possible solid solution between hurlbutite and strontiohurlbutite; such a solid solution is confirmed by the high Sr contents observed in some hurlbutite grains, reaching 10 wt% SrO.

## X-RAY POWDER DIFFRACTION

The X-ray powder diffraction pattern of strontiohurlbutite was collected using micro-diffraction data on 5 crystals, with a RIGAKU D/max Rapid IIR micro-diffractometer ( $\text{CuK}\alpha$ ,  $\lambda = 1.54056 \text{ \AA}$ ) at the School of Earth Sciences and Info-physics, Central South University, China. The micro-diffractometer was operated under these conditions: 48 kV, 250 mA, 0.05 mm collimator diameter, and 5 h exposure time. The hurlbutite-based structural model (Huminicki and Hawthorne 2002), in which Ca sites are occupied by Sr atoms, was used to index the powder diffraction data. Table 2 shows the main indexed micro-diffraction data of strontiohurlbutite. The stronger eight lines of the measured X-ray powder-diffraction pattern [ $d$  in  $\text{\AA}(hkl)$ ] are 3.554(100)(121); 3.355(51)(211); 3.073(38)(022); 2.542(67)(113); 2.230(42)(213); 2.215(87)(32 $\bar{1}$ ); 2.046(54)(223); 1.714(32)(143). The X-ray powder diffraction studies on the crystals of strontiohurlbutite gave the following unit-cell parameters:  $a = 8.005(4)$ ,  $b = 8.998(5)$ ,  $c = 8.426(5) \text{ \AA}$ ,  $\beta = 90.05(5)^\circ$ ,  $V = 606.9(3) \text{ \AA}^3$ ,  $Z = 4$ , and space group  $P2_1/c$ .

## CRYSTAL-STRUCTURE DETERMINATION

The X-ray intensity data, aimed to perform a structure refinement of strontiohurlbutite (CIF<sup>1</sup> available on deposit), were collected on an Agilent Technologies Xcalibur four-circle diffractometer, equipped with an EOS CCD area-detector (University of Liège, Belgium) on a crystal fragment measuring  $0.35 \times 0.35 \times 0.18 \text{ mm}$ . A total of 2186 frames with a spatial resolution of  $1^\circ$  were collected by the  $\varphi/\omega$  scan technique, with a counting time of 10 s per frame, in the range  $6.64^\circ < 2\theta < 58.18^\circ$ . A total of 26214 reflections were extracted from these frames, corresponding to 1566 unique reflections. Unit-cell parameters refined from these reflections are  $a = 7.997(1)$ ,  $b = 8.979(1)$ ,  $c = 8.420(1) \text{ \AA}$ ,  $\beta = 90.18(1)^\circ$ ,  $V = 604.7(1) \text{ \AA}^3$ , space group  $P2_1/c$ , in good agreement with those refined from the powder-diffraction data. A summary of the crystal data is presented in Table 3. The data were corrected for Lorenz, polarization, and absorption effects, the latter with an empirical method using the SCALE3 ABSPACK scaling algorithm included in the CrysAlisRED package (Oxford Diffraction 2007). The structure refinement

<sup>1</sup> Deposit item AM-14-204, CIF. Deposit items are stored on the MSA web site and available via the *American Mineralogist* Table of Contents. Find the article in the table of contents at GSW ([ammin.geoscienceworld.org](http://ammin.geoscienceworld.org)) or MSA ([www.minsocam.org](http://www.minsocam.org)), and then click on the deposit link.

TABLE 1. Representative electron-microprobe results of strontiohurlbutite from the Nanping No. 31 pegmatite dike

	Strontiohurlbutite from Nanping No. 31 pegmatite						Average	Ideal strontiohurlbutite
	NP-66 (zone I)		NP-14 (zone II)		NP-54 (zone IV)			
P <sub>2</sub> O <sub>5</sub> wt%	50.54	50.54	50.54	52.73	50.75	51.20	51.05	48.02
SrO	29.04	29.67	30.02	28.88	30.61	27.57	29.30	35.06
BeO*	17.71	17.71	17.71	17.71	17.71	17.71	17.71	16.92
CaO	0.07	0.17	0.15	0.18	1.80	3.10	0.91	
BaO	1.21	0.87	1.18	0.18	0.18	0.22	0.64	
Total	98.11	98.55	99.23	99.81	100.98	99.81	99.61	100.00
<b>Structural formulas calculated on the basis of O = 8 atoms</b>								
P apfu	2.051	2.047	2.043	2.087	2.025	2.036	2.048	2.000
Sr	0.807	0.823	0.831	0.783	0.837	0.751	0.805	1.000
Be	2.039	2.035	2.031	1.989	2.006	1.999	2.016	2.000
Ca	0.004	0.009	0.008	0.009	0.091	0.156	0.046	–
Ba	0.023	0.016	0.022	0.003	0.003	0.004	0.012	–

\* BeO was measured by SIMS.



was performed with anisotropic-displacement parameters for all atoms. The final conventional  $R_1$  factor [ $F_o > 2\sigma(F_o)$ ] is 0.0197. Atomic coordinates and anisotropic displacement parameters, as well as selected bond distances and angles, are given in Tables

4 and 5, respectively.

The structure of strontiohurlbutite is based on a tetrahedral framework consisting of corner-sharing  $\text{BeO}_4$  and  $\text{PO}_4$  tetrahedra (Fig. 3).  $\text{BeO}_4$  and  $\text{PO}_4$  tetrahedra are assembled in 4- and 8-membered rings, respectively. The 4-membered ring consists of a pair of tetrahedra pointing upward (U) and a pair of tetrahedra pointing downward (D), showing the UUDD type rings (Fig. 4a); the 8-membered ring shows the DDUDUUDU pattern (Fig. 4b). Sr atoms are localized in the channels formed by the alignment of the 8-membered rings (Fig. 3). A view perpendicular to the  $b$  direction shows that  $\text{BeO}_4$  and  $\text{PO}_4$  tetrahedra connected by corner-sharing form a double crankshaft chain running along  $a$  (Fig. 4c).

The  $\text{Sr}^{2+}$  ions are located in 10-coordinated polyhedra, characterized by 7 short bonds [ $\langle\text{Sr-O}\rangle = 2.596(2) \text{ \AA}$ ] and 3 long bonds [ $\langle\text{Sr-O}\rangle = 3.227(2) \text{ \AA}$ ]. This polyhedron can be described as a combination of a square pyramid and of a trigonal prism, with one square face in common. Based on the empirical parameters of Brown and Altermatt (1965), the bond-valence sums for strontiohurlbutite were calculated (Table 6). The bond-valence sums for P (5.00–5.04), Be (2.05–2.07), and Sr (2.09) are very close to the theoretical values.

The structure of strontiohurlbutite can be compared to those of hurlbutite (Mrose 1952; Bakakin and Belov 1959; Lindbloom et al. 1974) and paracelsian (Smith 1953; Bakakin and Belov 1960). The replacement of Ca in the structure of hurlbutite (effective ionic radius 1.06 Å; Shannon 1976) by Sr in strontiohurlbutite (effective ionic radius 1.21 Å) leads to an increase of the seven shorter  $M^{2+}\text{-O}$  bonds from 2.469(6) to 2.596(2) Å, respectively. This larger crystallographic site also implies an increase of the unit-cell parameters of strontiohurlbutite, compared to those of hurlbutite (Table 7).

ORIGIN AND IMPLICATIONS

Strontium is a widespread element in most rocks. Since its crystal-chemistry is similar to that of calcium, Sr commonly substitutes for Ca in minerals, especially in phosphates. Various Sr-bearing phosphate minerals, including stronadelphite (Pekov et al. 2010), palermoite (Mrose 1953; Ni et al. 1993), goedkenite (Moore et al. 1975), and strontiohurlbutite (Britvin et al. 1991), are known to have a Ca-bearing isostructural analog. The new mineral species described in the present paper, strontiohurlbutite, is the Sr-dominant analog of hurlbutite, and constitutes a new member of the hurlbutite group (Table 7).

Strontiohurlbutite occurs in close association with hurlbu-

TABLE 2. Powder X-ray diffraction data for strontiohurlbutite

<i>h</i>	<i>k</i>	<i>l</i>	<i>d</i> <sub>meas</sub> (Å)	<i>d</i> <sub>calc</sub> (Å)	<i>I</i> <sub>rel</sub>
0	1	1	6.150	6.150	9
1	1	0	5.985	5.981	3
2	1	0	3.653	3.657	5
1	2	1	3.554	3.555	100
2	1	1	3.355	3.354	51
0	2	2	3.073	3.075	38
1	3	0	2.810	2.809	27
0	1	3	2.678	2.681	9
1	1	3	2.542	2.542	67
0	2	3	2.380	2.383	26
3	2	0	2.294	2.295	1
2	1	3	2.230	2.227	42
3	2	1	2.215	2.215	87
2	3	2	2.083	2.086	26
2	2	3	2.046	2.047	54
3	3	0	1.994	1.994	19
1	1	4	1.986	1.986	13
3	2	3	1.776	1.777	16
2	2	4	1.721	1.722	21
1	4	3	1.714	1.715	32
0	1	5	1.655	1.656	11
3	1	4	1.627	1.627	31
3	1	4	1.623	1.625	6
1	2	5	1.549	1.549	10
4	2	3	1.531	1.532	4
5	1	3	1.376	1.375	6

TABLE 3. Crystal data and refinement parameters for strontiohurlbutite

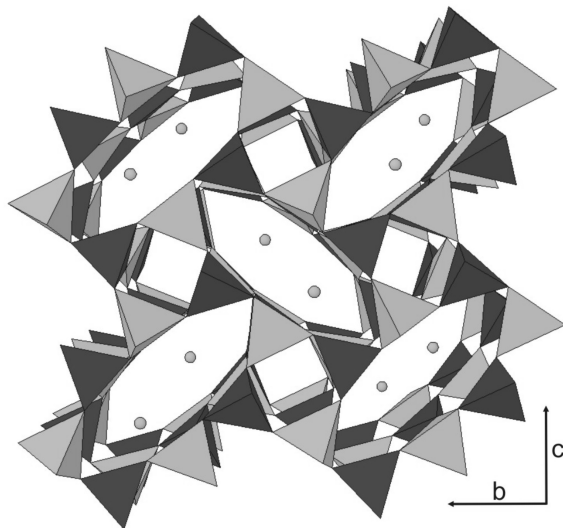
Crystal size (mm)	0.35 × 0.35 × 0.18
Color	Light blue
Space group	$P2_1/c$
<i>a</i> , <i>b</i> , <i>c</i> (Å)	7.997(1), 8.979(1), 8.420(1)
$\beta$ (°)	90.18(1)
<i>V</i> (Å <sup>3</sup> )	604.7(1)
<i>Z</i>	4
<i>D</i> (calc) (g/cm <sup>3</sup> )	3.101
$2\theta_{\text{min}}$ – $2\theta_{\text{max}}$	6.64°–58.18°
Range of indices	$-10 \leq h \leq 10, -12 \leq k \leq 12, -11 \leq l \leq 11$
Measured intensities	26214
Unique reflections	1566
Independent non-zero [ $I > 2\sigma(I)$ ] reflections	1473
$\mu$ (mm <sup>-1</sup> )	9.451
Refined parameters	118
$R_1$ [ $F_o > 2\sigma(F_o)$ ]	0.0197
$R_1$ (all)	0.0234
$wR_2$ (all)	0.0467
<i>S</i> (goodness of fit)	1.106
Max $\Delta/\sigma$ in the last l.s. cycle	0.001
Max peak and hole in the final $\Delta F$ map (e/Å <sup>3</sup> )	+0.44 and -0.42

TABLE 4. Atomic coordinates and displacement parameters (Å<sup>2</sup>) for strontiohurlbutite

Atom	<i>x</i>	<i>y</i>	<i>z</i>	<i>U</i> <sub>11</sub>	<i>U</i> <sub>22</sub>	<i>U</i> <sub>33</sub>	<i>U</i> <sub>23</sub>	<i>U</i> <sub>13</sub>	<i>U</i> <sub>12</sub>	<i>U</i> <sub>eq</sub>
Sr	0.25553(2)	0.91255(2)	0.10887(2)	0.0093(1)	0.0075(1)	0.0092(1)	-0.00060(7)	-0.00046(7)	0.00024(7)	0.00867(7)
P1	0.56332(7)	0.69579(6)	-0.06627(6)	0.0073(2)	0.0049(2)	0.0049(2)	0.0001(2)	-0.0002(2)	0.0001(2)	0.0057(1)
P2	0.06219(7)	0.58553(6)	0.23174(6)	0.0070(2)	0.0060(2)	0.0046(2)	-0.0003(2)	-0.0004(2)	-0.0002(2)	0.0059(1)
Be1	0.4288(3)	0.9193(3)	-0.2734(3)	0.009(1)	0.008(1)	0.008(1)	0.000(1)	-0.000(1)	0.001(1)	0.0080(5)
Be2	-0.0739(3)	0.6931(3)	-0.0633(3)	0.009(1)	0.009(1)	0.007(1)	0.001(1)	-0.001(1)	-0.000(1)	0.0084(5)
O1	0.4369(2)	0.6818(2)	0.0703(2)	0.0101(7)	0.0093(7)	0.0075(7)	0.0009(6)	0.0014(6)	0.0008(6)	0.0090(3)
O2	0.2404(2)	0.9069(2)	-0.1991(2)	0.0074(7)	0.0162(8)	0.0071(7)	0.0005(6)	0.0000(6)	-0.0004(6)	0.0102(3)
O3	0.5490(2)	0.8580(2)	-0.1277(2)	0.0106(7)	0.0062(7)	0.0082(7)	0.0018(6)	-0.0025(6)	0.0001(6)	0.0083(3)
O4	0.7383(2)	0.6626(2)	-0.0085(2)	0.0082(7)	0.0111(8)	0.0119(7)	0.0029(6)	-0.0001(6)	-0.0003(6)	0.0104(3)
O5	0.4906(2)	1.0885(2)	-0.3003(2)	0.0143(7)	0.0067(7)	0.0074(7)	0.0018(5)	-0.0028(6)	-0.0011(6)	0.0095(3)
O6	-0.0063(2)	0.9273(2)	0.3062(2)	0.0141(8)	0.0062(7)	0.0084(7)	0.0009(5)	0.0023(6)	0.0007(6)	0.0096(3)
O7	0.0564(2)	0.6876(2)	0.0871(2)	0.0102(7)	0.0087(7)	0.0068(7)	0.0015(6)	-0.0020(6)	-0.0014(6)	0.0085(3)
O8	-0.0555(2)	0.8622(2)	-0.1352(2)	0.0090(7)	0.0067(7)	0.0084(7)	0.0017(6)	0.0022(6)	0.0004(6)	0.0080(3)

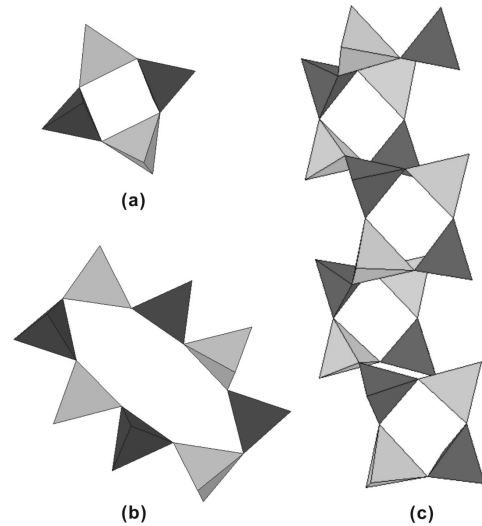
**TABLE 5.** Selected bond distances (Å) and angles (°) for strontiohurlbutite

P1-O3	1.549(2)	O2-Be1-O3	103.2(2)
P1-O5	1.541(2)	O5-Be1-O2	113.6(2)
P1-O4	1.509(2)	O5-Be1-O3	103.9(2)
P1-O1	1.538(2)	O1-Be1-O2	108.4(2)
Mean	1.535	O1-Be1-O3	113.4(2)
		O1-Be1-O5	113.9(2)
		Mean	109.39
O5-P1-O3	108.92(8)	Be2-O8	1.642(3)
O4-P1-O3	111.16(9)	Be2-O7	1.638(3)
O4-P1-O5	111.62(9)	Be2-O4	1.597(3)
O4-P1-O1	110.68(8)	Be2-O6	1.635(3)
O1-P1-O3	106.14(8)	Mean	1.628
O1-P1-O5	108.12(9)	O7-Be2-O8	104.8(2)
Mean	109.44	O7-Be2-O8	110.6(2)
P2-O8	1.539(2)	O7-Be2-O8	111.6(2)
P2-O2	1.540(2)	O7-Be2-O8	113.2(2)
P2-O7	1.525(2)	O7-Be2-O8	109.5(2)
P2-O6	1.523(2)	O7-Be2-O8	106.8(2)
Mean	1.531	Mean	109.40
O8-P2-O2	106.21(8)	Sr-O8	2.588(2)
O7-P2-O8	112.43(9)	Sr-O8'	3.253(2)
O7-P2-O2	107.53(9)	Sr-O2	3.295(2)
O6-P2-O8	104.89(9)	Sr-O2'	2.596(2)
O6-P2-O2	113.03(9)	Sr-O3	2.591(2)
O6-P2-O7	112.64(9)	Sr-O3'	3.122(2)
Mean	109.45	Sr-O5	2.588(2)
		Sr-O7	2.579(2)
Be1-O2	1.637(3)	Sr-O6	2.680(2)
Be1-O3	1.651(3)	Sr-O1	2.551(2)
Be1-O5	1.614(3)	Mean	2.784
Be1-O1	1.600(3)		
Mean	1.627		

**FIGURE 3.** The crystal structure of strontiohurlbutite. Note: PO<sub>4</sub> tetrahedra in dark gray; BeO<sub>4</sub> tetrahedra in gray; circle for Sr atoms.

tite, thus indicating that both minerals may crystallize under a comparable range of physicochemical conditions. Their textural relationships suggest that the hurlbutite-group minerals evolved from hurlbutite to strontiohurlbutite. Strontiohurlbutite crystals are enriched in Ba in zones I–II and in Ca in zone IV (Table 1), thus indicating a solid solution with hurlbutite. Consequently, the activity of Sr in the pegmatite fluids seems to be an essential factor controlling the crystallization of strontiohurlbutite.

High-Sr activity in late hydrothermal fluids affecting pegma-

**FIGURE 4.** Chains and rings in the crystal structure of strontiohurlbutite (PO<sub>4</sub> tetrahedra = dark gray; BeO<sub>4</sub> tetrahedra = gray). (a) 4-membered ring with the pattern UUDD; (b) 8-membered ring with the pattern DDUDUUDU; (c) double-crankshaft chain aligned along the *a* axis.**TABLE 6.** Bond valence sums for strontiohurlbutite

	Sr	P1	P2	Be1	Be2	Σ
O1	0.31	1.23		0.55		2.10
O2	0.27					
	0.04		1.23	0.50		2.05
O3	0.28					
	0.07	1.20		0.48		2.03
O4		1.33			0.56	1.89
O5	0.28	1.23		0.53		2.04
O6	0.22		1.29		0.50	2.01
O7	0.29		1.28		0.50	2.07
O8	0.28					
	0.05		1.23		0.49	2.06
Σ	2.09	5.00	5.04	2.07	2.05	

**TABLE 7.** Comparison of the physical properties of strontiohurlbutite and hurlbutite

	Strontiohurlbutite	Hurlbutite (Mrose 1952)
Color	light blue	colorless to greenish
Structural formula	SrBe <sub>2</sub> (PO <sub>4</sub> ) <sub>2</sub>	CaBe <sub>2</sub> (PO <sub>4</sub> ) <sub>2</sub>
Space group	<i>P</i> 2 <sub>1</sub> / <i>c</i>	<i>P</i> 2 <sub>1</sub> / <i>a</i>
<i>a</i>	7.997(1) Å	8.29 Å
<i>b</i>	8.979(1) Å	8.80 Å
<i>c</i>	8.420(1) Å	7.81 Å
β	90.18(1)°	90.5°
<i>V</i>	604.7(1) Å <sup>3</sup>	570 Å <sup>3</sup>
<i>Z</i>	4	4
Density	3.101 <sup>a</sup> g/cm <sup>3</sup> (calc)	2.90 <sup>a</sup> g/cm <sup>3</sup> (calc)

<sup>a</sup> Density calculation based on the empirical formula.

tite systems was documented in the literature (e.g., Moore 1982; Charoy et al. 2003). This high activity induces the replacement of early minerals by secondary Sr-bearing minerals such as palermoite and goyazite (e.g., Ni et al. 1993; Galliski et al. 2012). In the Nanping No. 31 pegmatite, strontiohurlbutite occurs with hurlbutite along fractures of primary beryl (Fig. 1c); this petrographic texture indicates that the primary beryl was affected by a late Sr-, Ca-, and P-rich hydrothermal fluid. Hurlbutite contains high SrO contents, from 5 to 10 wt%, thus indicating that Sr in

the late hydrothermal fluids became a trigger for the transition from hurlbutite to strontiohurlbutite. In fact, other secondary Sr-bearing phosphate minerals such as palermoite, goyazite, hydroxylapatite, and bertossaite were found in the Nanping No. 31 pegmatite (Ni et al. 1993; Yang et al. 1994); the source of Sr in the hydrothermal fluids, responsible for the crystallization of these secondary minerals, remains to be determined in the future.

#### ACKNOWLEDGMENTS

Financial support for the research was provided by NSF of China (Grant No. 41102020, 41230315), the Ministry of Science and Technology (Grant No. 2012CB416704), and by the Fundamental Research Funds for the Central Universities. We are indebted to CHEN Guojian (Geological Survey of North Fujian) for his help during fieldwork.

#### REFERENCES CITED

- Bakakin, V.V., and Belov, N.V. (1959) The crystalline structure of hurlbutite. *Doklady Akademii Nauk SSSR*, 125, 343–344.
- (1960) Crystal structure of paracelsian. *Soviet Physics Crystallography*, 5, 826–829.
- Britvin, S.N., Pakhomovskii, Y.A., Bogdanova, A.N., and Skiba, V.I. (1991) Strontiohurlbutite,  $\text{Sr}_3\text{Mg}(\text{PO}_3\text{OH})(\text{PO}_4)_6$ , a new mineral species from the Kovdor Deposit, Kola Peninsula, U.S.S.R. *Canadian Mineralogist*, 29, 87–93.
- Brown, I.D., and Altermatt, D. (1965) Bond-valence parameters obtained from a systematic analysis of the inorganic crystal structure database. *Acta Crystallographica*, B41, 244–247.
- Charoy, B., Chaussidon, M., Carlier De Veslud, C.L., and Duthou, J.L. (2003) Evidence of Sr mobility in and around the albite-lepidolite-topaz granite of Beauvoir (France): an in-situ ion and electron probe study of secondary Sr-rich phosphates. *Contributions to Mineralogy and Petrology*, 145, 673–690.
- Galliski, M.A., Černý, P., Márquez-Zavalía, M.F., and Chapman, R. (2012) An association of secondary Al-Li-Be-Ca-Sr phosphates in the San Elias pegmatite, San Luis, Argentina. *Canadian Mineralogist*, 50, 933–942.
- Hatert, F., Ottolini, L., and Schmid-Beurmann, P. (2011) Experimental investigation of the alluaudite + triphylite assemblage, and development of the Nan-in-triphylite geothermometer: applications to natural pegmatite phosphates. *Contributions to Mineralogy and Petrology*, 161, 531–546.
- Huminicki, D.M.C., and Hawthorne, F.C. (2002) The crystal chemistry of the phosphate minerals. In M.L. Kohn, J. Rakovan, and J.M. Hughes, Eds., *Phosphates—Geochemical, Geobiological, and Materials Importance*, 48, p. 123–253. *Reviews in Mineralogy and Geochemistry*, Mineralogical Society of America, Chantilly, Virginia.
- Lindbloom, J.T., Gibbs, G.V., and Ribbe, P.H. (1974) The crystal structure of hurlbutite: a comparison with danburite and anorthite. *American Mineralogist*, 59, 1267–1271.
- Mandarino, J.A. (1981) The Gladstone-Dale relationship. IV. The compatibility concept and its application. *Canadian Mineralogist*, 19, 441–450.
- Moore, P.B. (1982) Pegmatite minerals of P(V) and B(III). In P. Černý, Ed., *Granitic Pegmatites in Science and Industry*. Mineralogical Association of Canada Short Course Handbook E, p. 267–291.
- Moore, P.B., Irving, A.J., and Kampf, A.R. (1975) Foggite,  $\text{CaAl}(\text{OH})_2(\text{H}_2\text{O})[\text{PO}_4]$ ; goedkenite,  $(\text{Sr,Ca})_2\text{Al}(\text{OH})[\text{PO}_4]_2$ ; and samuelsonite,  $(\text{Ca,Ba})\text{Fe}_2^{2+}\text{Mn}_2^{2+}\text{Ca}_8\text{Al}_2(\text{OH})_2[\text{PO}_4]_{10}$ ; three new species from the Palermo No. 1 pegmatite, North Groton, New Hampshire. *American Mineralogist*, 60, 957–964.
- Mrose, M.E. (1952) Hurlbutite,  $\text{CaBe}_2(\text{PO}_4)_2$ , a new mineral. *American Mineralogist*, 37, 931–940.
- (1953) Palermoite and goyazite, two strontium minerals from the Palermo mine, North Groton, N.H. (abstr.). *Proceedings of the thirty-third annual meeting of The Mineralogical Society of America at Boston, Massachusetts*, *American Mineralogist*, 38, p. 354.
- Ni, Y.X., Yang, Y.Q., and Wang, W.Y. (1993) Palermoite-bertossaite in Nanping granitic pegmatites, Fujian. *Acta Mineralogica Sinica*, 13, 346–353 (in Chinese with English abstract).
- Ottolini, L., Bottazzi, P., and Vannucci, R. (1993) Quantification of lithium, beryllium and boron in silicates by secondary ion mass spectrometry using conventional energy filtering. *Analytical Chemistry*, 65, 1960–1968.
- Ottolini, L., Cámara, F., Hawthorne, F.C., and Stirling, J. (2002) SIMS matrix effects in the analysis of light elements in silicate minerals: Comparison with SREF and EMPA data. *American Mineralogist*, 87, 1477–1485.
- Oxford Diffraction (2007) *CrysAlis CCD and CrysAlis RED*, vers. 1.71. Oxford Diffraction, Oxford, U.K.
- Pekov, I.V., Britvin, S.N., Zubkova, N.V., Pushcharovsky, D.Y., Pasero, M., and Merlino, S. (2010) Stronadelphite,  $\text{Sr}_3(\text{PO}_4)_3\text{F}$ , a new apatite-group mineral. *European Journal of Mineralogy*, 22, 869–874.
- Rao, C., Wang, R.C., Hu, H., and Zhang, W.L. (2009) Complex internal textures in oxide minerals from the Nanping No. 31 dyke of granitic pegmatite, Fujian province, Southeastern China. *Canadian Mineralogist*, 47, 1195–1212.
- Rao, C., Wang, R.C., and Hu, H. (2011) Paragenetic assemblages of beryllium silicates and phosphates from the Nanping no. 31 granitic pegmatite dyke, Fujian province, southeastern China. *Canadian Mineralogist*, 49, 1175–1187.
- Shannon, R.D. (1976) Revised effective ionic radii and systematic studies of interatomic distances in halides and chalcogenides. *Acta Crystallographica*, A32, 751–767.
- Smith, J.V. (1953) The crystal structure of paracelsian,  $\text{BaAl}_2\text{Si}_2\text{O}_8$ . *Acta Crystallographica*, 6, 613–620.
- Williams, P.A., Hatert, F., Pasero, M., and Mills, S.J. (2012) New minerals and nomenclature modifications approved in 2012. *Mineralogical Magazine*, 76, 807–817.
- Yang, Y.Q., Ni, Y.X., Guo, Y.Q., Qiu, N.M., Chen, C.H., Cai, C.F., Zhang, Y.P., Liu, J.B., and Chen, Y.X. (1987) Rock-forming and ore-forming characteristics of the Xikeng granitic pegmatites in Fujian Province. *Mineral Deposits*, 6(3), 10–21 (in Chinese with English abstract).
- Yang, Y.Q., Wang, W.Y., Lin G.X., Chen, C.H., and Zhu, J.H. (1994) Phosphate minerals and their geochemical evolution of granitic pegmatite in Nanping, Fujian Province. *Geology of Fujian*, 13(4), 215–226 (in Chinese with English abstract).

MANUSCRIPT RECEIVED MARCH 26, 2013

MANUSCRIPT ACCEPTED SEPTEMBER 23, 2013

MANUSCRIPT HANDLED BY FERNANDO COLOMBO